
Article:
Marín-Márquez, C. orcid.org/0000-0002-9444-7852, Adisa, A.O., Niklander, S.E. et al. (2 more authors) (2025) Genomic and transcriptomic analysis of ameloblastoma reveals distinct molecularly aggressive phenotypes. Modern Pathology, 38 (3). 100682. ISSN 0893-3952

https://doi.org/10.1016/j.modpat.2024.100682

Supplementary Material for

Genomic and transcriptomic analysis of ameloblastoma reveals distinct molecularly aggressive phenotypes

WES Library construction and sequencing performed at Novogene

Sequencing libraries were generated using Agilent Sure Select Human All ExonV6 kit (Agilent Technologies, CA, USA) following manufacturer's recommendations and x index codes were added to attribute sequences to each sample. Fragmentation was carried out by hydrodynamic shearing system (Covaris, Massachusetts, USA) to generate 180-280 bp fragments.

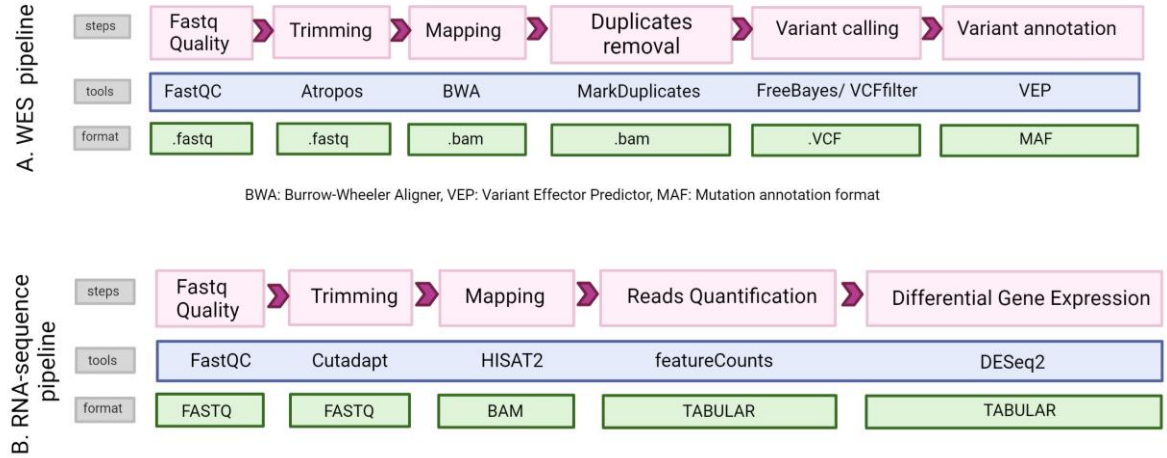

Supplementary Figure S1A and S1B: Processing of raw sequencing data from WES and RNA-sequencing

From VCF to MAF

The script was found in https://github.com/mskcc/vcf2maf/tree/v1.6.16

perl vcf2maf.pl --input-vcf tests/test.vcf --output-maf tests/test.vep.maf

Pathway enrichment analysis

For the Pathway enrichment analysis and visualization, the protocol stated by Reimand et al. was followed, and consisted of three main steps:

- *Definition of the gene list of interest.* For the analysis of the genes from WES, pathway enrichment analysis was performed from the list of genes with the variants obtained from Phase 2 Stage 1 of the workflow shown in Figure 1.
- *Pathway enrichment analysis using g:Profiler.* This list was uploaded to the open web server tool, g:Profiler (https://biit.cs.ut.ee/gprofiler/gost) [1].

- *Visualization and Interpretation of the pathway enrichment analysis results.* The Enrichment map was created with Cytoscape 3.9.1 Desktop [2].

RNA sequencing Library construction and sequencing performed at Novogene

One sample failed the quality control test (one tumour sample-T31), therefore sixteen samples continued with the library preparation and sequencing. The qualified libraries are fed into Illumina sequencers after pooling according to its effective concentration and expected data volume.

Molecular Analysis

Polymerase chain reaction (PCR)

Total DNA was extracted from tumours by manual macro-dissection, using QIAamp DNA Mini Kit (QIAGEN, Germany) following manufacturer's instructions and quantified using a NanoDrop spectrophotometer. 2X PCRBIO VeriFi Mix Red (PCR Bio Systems, UK) was used for the PCR following the manufacturer's instructions using a Peltier Thermal cycler (MJ Research, UK). The details of the cycles are listed in Supplementary Table S1. Amplicons generated by PCR were separated on TAE-agarose gel electrophoresis, using 1-2% agarose gels with 0.5- 1 µl/100 ml ethidium bromide. 20 µl of each sample was loaded into the wells. A 1000 bp ladder (PCRBIO Ladder IV, PCR Bio Systems) was used as a reference marker. Samples were electrophoresed for 30-45 min at 80-120 v and visualized under UV transillumination in a G-BOX (Syngene, UK) using the GeneSys image acquisition software (Syngene, UK).

Gels were visualized under a UV transillumination box in a special room and around 100 mg of each DNA band was cut with a sterile razor blade from the gels and placed in labeled Eppendorf tubes. Using Isolate II PCR and Gel Kit (Bioline, UK), the DNA was purified from gels following the manufacturer's instructions, and then a 1.5% TAE-agarose gel was run to check that the DNA was properly purified.

Supplementary Table S1: Details of thermal cycler setting for PCR

	1 cycle	**30 cycles**		
Temp (°C)	95	95	65	72
Time	1 min	15 secs	15 secs	30 secs

Quantitative PCR (qPCR)

All reactions were performed in total volumes of 10 µl (9 µl of the master mix, plus 1 µl of cDNA). The standard thermal cycle stings for a reaction consisted of 40 cycles. One cycle consisted of 95°C for 10 seconds, 60°C for 15 seconds and 72°C for 20 seconds. TaqMan probes for CTNNB1 and TGM2 were bought from Thermo Fisher Scientific, Cambridge, UK. Predesigned PrimeTime® qPCR Assays for KMT2D and SERPINB3 were bought from Integrated DNA Technologies (IDT). The oligonucleotides for LAPTM5 were designed in-house and bought from Sigma- Aldrich, Gillingham, UK. Primer Blast was used to examine primer specificity (https://www.ncbi.nlm.nih.gov/tools/primer-blast/).

Supplementary Table S2: Details of probes, assays and oligonucleotides for qPCR

TaqMan probe	Reference (Hs number)	RefSeq Number	Exon Boundary
CTNNB1	00994404_g1	NM_001098209.1	1-2
	00355045_m1		10- 11
TGM2	01096681_m1	NM_001323316.1	9- 10
IDT Assay Name	**Gene name**	**RefSeq Number**	**Exon Boundary**
Hs.PT.58.40598446.gs	*KMT2D*	NM_003482	5-6
Hs.PT.58.15069322.gs	*SERPINB3*	NM_00919	1-2
Gene	**RefSeq**	**Oligonucleotide Sequence (Forward/Reverse)**	**Exon Boundary**
LAPTM5	NM_006762.3	5' -TGCTTCAATGTCCGCATCGC-3' 5' -TTGCCATGGGCCACCTCTAC-3'	1-2

Supplementary Table S3: WES pipeline output from Phase 1 and 2

		Number of variants			
Sample	**Raw VCF**	**PHASE 1. Stage 1** (FP)	**PHASE 1. Stage 2** (FCS)	**PHASE 2. Stage 1** (AV)	**PHASE 2. Stage 1** (NAV)
T8	26500	1840	659	17	506
T9	25769	1767	596	18	464
T10	26192	1727	629	25	507
T11	27699	1965	608	17	450
T12	27043	1819	613	29	470
T13	26303	1699	581	22	433
T16	26959	1746	582	20	432
T17	27107	1892	645	29	495
T19	25933	1818	635	26	476
T26	26282	1872	604	28	459
T29	26025	1730	585	25	431
T30	27466	2013	687	16	533
T31	26282	1756	622	17	483

VCF: variant calling format; FP: filtering by population; FCS: filtering by clinical significance; AV: annotated variants; NAV: non-annotated variants.

Supplementary Table S4: Somatic variants in ameloblastoma

Hugo Symbol	Start Position	End Position	Variant Classification	Reference Allele	Tumor Seq Allele1	Tumor Seq Allele2	dbSNP_RS	Sample	AA change
IGHMBP2	68908153	68908153	Missense	G	G	A	rs1384314579	S8	p.V89M
ZNF705E	71819721	71819721	Missense	C	C	T	rs11235129	S8	p.W21*
WDHD1	55010375	55010375	Missense	C	C	T	rs775370465	S8	p.R92H
ADAMTS7	78771767	78771767	Missense	C	C	T	rs759491085	S8	p.E732K
LILRB2	54279040	54279040	Missense	G	G	A	rs1473278082	S8	p.L243F
OTOP1	4188965	4188965	Missense	T	T	C		S8	p.I559M
ICE1	5468936	5468936	Missense	G	G	A	rs181505478	S8	p.R2057H
HLA-DRB5	32530124	32530124	Splice_Site	C	C	G	rs79192142	S8	p.X34_splice
DNAJC30	73683218	73683218	Missense	T	T	G		S8	p.Y69S
RBM28	1.28E+08	1.28E+08	Missense	G	G	A	rs1168195672	S8	p.R119W
SLC25A5	1.19E+08	1.19E+08	Missense	T	T	A	rs780390657	S8	p.F82I
FCGBP	39899549	39899549	Splice_Region	C	C	T	rs1157993436	S8	
PRSS3P1	1.43E+08	1.43E+08	Splice_Region	G	G	A	rs555702549	S8	
NBPF12	1.47E+08	1.47E+08	Missense	A	A	T	rs1553886396	S9	p.N492I
NBPF11	1.48E+08	1.48E+08	Missense	T	T	C	rs57784339	S9	p.N53S
OR13A1	45304502	45304502	Splice_Site	T	T	G	rs10900195	S9	
INCENP	62141015	62141015	Missense	C	C	T	rs747966600	S9	p.R522C
OR5BS1P	48560442	48560442	Missense	G	G	C	rs7312017	S9	p.L187F
ARHGEF7	1.11E+08	1.11E+08	Missense	G	G	A	rs768509936	S9	p.R278Q
LILRB2	54279040	54279040	Missense	G	G	A	rs1473278082	S9	p.L243F
ABCF3	1.84E+08	1.84E+08	Missense	C	C	T	rs751570547	S9	p.R596W
BRAF	1.41E+08	1.41E+08	Missense	A	A	T	rs113488022	S9	p.V640E
FCGBP	39899549	39899549	Splice_Region	C	C	T	rs1157993436	S9	
ATP8A1	42446650	42446650	Splice_Region	C	C	T	rs761497932	S9	
MUC3A	1.01E+08	1.01E+08	Splice_Region	G	G	A	rs75534608	S9	

NBPF12	1.47E+08	1.47E+08	Missense	A	A	T	rs1553886396	S10	p.N492I
CHIT1	2.03E+08	2.03E+08	Missense	C	C	T		S10	p.G37R
OR13A1	45304502	45304502	Splice_Site	T	G	G	rs10900195	S10	
ZNF705E	71819721	71819721	Nonsense	C	C	T	rs11235129	S10	p.W21*
TAS2R19	11022273	11022273	Missense	G	G	C		S10	p.A100G
OR5BS1P	48560442	48560442	Missense	G	G	C	rs7312017	S10	p.L187F
AKAP6	32824051	32824051	Nonsense	G	G	T		S10	p.E2080*
AKT1	1.05E+08	1.05E+08	Missense	C	C	T	rs121434592	S10	p.E17K
ZNF106	42422608	42422608	Missense	C	C	T	rs377219331	S10	p.V1756M
UBR1	43024846	43024846	Nonsense	C	C	A		S10	p.E908*
KCNN1	17974183	17974183	Missense	C	C	G		S10	p.L99V
LILRB2	54279040	54279040	Missense	G	G	A	rs1473278082	S10	p.L243F
BIRC6	32442201	32442201	Missense	G	G	A		S10	p.G1361R
LRP1B	1.41E+08	1.41E+08	Missense	C	C	T	rs764483142	S10	p.G2385R
SRA1	1.41E+08	1.41E+08	In_Frame_Ins	C	C	GTCG	rs368142622	S10	p.V110delinsRL
BRAF	1.41E+08	1.41E+08	Missense	A	A	T	rs113488022	S10	p.V640E
SWI5	1.28E+08	1.28E+08	Missense	G	G	T	rs199960390	S10	p.L160F
SLC25A5	1.19E+08	1.19E+08	Missense	T	T	A	rs780390657	S10	p.F82I
SLC25A5	1.19E+08	1.19E+08	Nonsense	G	G	T	rs73213195	S10	p.E293*
PCMTD2	64260271	64260271	Splice_Region	A	A	G	rs942944758	S10	p.L102=
SRA1	1.41E+08	1.41E+08	Splice_Region	GGT	GGT	A	rs1554096269	S10	
OR13A1	45304502	45304502	Splice_Site	T	T	G	rs10900195	S11	
AGAP9	47502579	47502579	Missense	C	C	T	rs1283007591	S11	p.R517Q
OR51A7	4908217	4908217	Missense	C	C	T	rs376011053	S11	p.P283L
AHNAK	62522127	62522127	Missense	T	T	C		S11	p.D4097G
SLCO1B3	20877891	20877891	Missense	G	G	C		S11	p.E364Q
DNAH10	1.24E+08	1.24E+08	Missense	G	G	A	rs1360251097	S11	p.D3555N
ANKRD12	9258461	9258461	Missense	C	C	T	rs1014443518	S11	p.P1732S
LILRB2	54279040	54279040	Missense	G	G	A	rs1473278082	S11	p.L243F
KIF3B	32331300	32331300	Missense	G	G	A	rs867330475	S11	p.R742Q

QRFPR	1.21E+08	1.21E+08	Missense	G	G	A	rs541376457	S11	p.P41L
CSF1R	1.5E+08	1.5E+08	Missense	C	C	T	rs281860271	S11	p.A770T
SAMD3	1.3E+08	1.3E+08	Missense	G	G	T		S11	p.S283Y
BRAF	1.41E+08	1.41E+08	Missense	A	A	T	rs113488022	S11	p.V640E
FCGBP	39899549	39899549	Splice_Region	C	C	T	rs1157993436	S11	
MUC3A	1.01E+08	1.01E+08	Splice_Region	G	G	A	rs75534608	S11	
EXTL3	28713449	28713449	Splice_Region	T	T	A	rs528490258	S11	
TMEM269	42793651	42793651	Missense	G	G	A	rs926584310	S12	p.A106T
CFAP57	43254138	43254138	Missense	C	C	T	rs966708758	S12	p.R1267W
GFI1	92476055	92476055	Missense	G	G	A	rs781101695	S12	p.R415W
OR13A1	45304502	45304502	Splice_Site	T	T	G	rs10900195	S12	
GPR18	99255706	99255706	Missense	G	G	A	rs753458670	S12	p.T56M
HEATR5A	31371853	31371853	Missense	G	G	A	rs750697233	S12	p.R640C
RGMA	93052109	93052109	Missense	G	G	A	rs764968962	S12	p.R185C
BEST2	12752666	12752666	Missense	G	G	T		S12	p.R25L
LILRB2	54279040	54279040	Missense	G	G	A	rs1473278082	S12	p.L243F
GALNT14	30945861	30945861	Missense	G	G	A	rs761709195	S12	p.R227W
ANKZF1	2.19E+08	2.19E+08	Missense	G	G	A	rs376327826	S12	p.V208M
CTNNB1	41224610	41224610	Missense	C	C	A	rs121913400	S12	p.S33Y
SRA1	1.41E+08	1.41E+08	In_Frame_Ins	C	C	GTCG	rs368142622	S12	p.V110delinsRL
BRAF	1.41E+08	1.41E+08	Missense	A	A	T	rs113488022	S12	p.V640E
OGT	71537918	71537918	Missense	G	C	C		S12	p.G103A
SLC25A5	1.19E+08	1.19E+08	Missense	T	T	A	rs780390657	S12	p.F82I
ANKRD30A	37145060	37145060	Splice_Region	T	T	C	rs200031600	S12	
FCGBP	39899549	39899549	Splice_Region	C	C	T	rs1157993436	S12	
SRA1	1.41E+08	1.41E+08	Splice_Region	GGT	GGT	A	rs1554096269	S12	
MUC3A	1.01E+08	1.01E+08	Splice_Region	G	G	A	rs75534608	S12	
TPR	1.86E+08	1.86E+08	Missense	G	G	C	rs1387480848	S13	p.Q1162E
OR13A1	45304502	45304502	Splice_Site	T	T	G	rs10900195	S13	
OTOG	17561764	17561764	Missense	C	C	T	rs940869941	S13	p.S546L

ZNF705E	71819721	71819721	Nonsense	C	C	T	rs11235129	S13	p.W21*
KRT18	52949447	52949447	Missense	G	G	C	rs1434610693	S13	p.A92P
MYO1E	59261484	59261484	Missense	G	G	A		S13	p.S58L
ABHD15	29562920	29562920	Missense	C	C	T	rs374284598	S13	p.V350M
DNAH17	78486406	78486406	Missense	G	G	A	rs779251038	S13	p.R2307C
KANK2	11193823	11193823	Missense	G	G	A	rs746508563	S13	p.S86L
LILRB2	54279040	54279040	Missense	G	G	A	rs1473278082	S13	p.L243F
CTNNB1	41224610	41224610	Missense	C	C	G	rs121913400	S13	p.S33C
SI	1.65E+08	1.65E+08	Missense	C	C	T	rs773389871	S13	p.R588H
SRA1	1.41E+08	1.41E+08	In_Frame_Ins	C	GTCG	GTCG	rs368142622	S13	p.V110delinsRL
ANKRD30A	37145060	37145060	Splice_Region	T	T	C	rs200031600	S13	
SRA1	1.41E+08	1.41E+08	Splice_Region	GGT	A	A	rs1554096269	S13	
NBPF12	1.47E+08	1.47E+08	Missense	A	A	T	rs1553886396	S16	p.N492I
ZNF705E	71819721	71819721	Nonsense	C	C	T	rs11235129	S16	p.W21*
MYO1A	57046604	57046604	Missense	C	C	A	rs1276414495	S16	p.R196S
UBE3B	1.1E+08	1.1E+08	Missense	A	A	C		S16	p.S810R
ATP4A	35555679	35555679	Missense	C	C	T	rs145767701	S16	p.R668H
LILRB2	54279040	54279040	Missense	G	G	A	rs1473278082	S16	p.L243F
OSBP2	30741311	30741311	Missense	G	G	C	rs145882890	S16	p.W265C
CFAP97	1.85E+08	1.85E+08	Missense	C	C	A		S16	p.D194Y
HBEGF	1.4E+08	1.4E+08	Missense	G	G	A		S16	p.R128W
NPTX2	98624966	98624966	Missense	C	C	G		S16	p.P230A
BCOR	40062246	40062246	Nonsense	G	G	A		S16	p.Q1441*
SLC25A5	1.19E+08	1.19E+08	Missense	T	T	A	rs780390657	S16	p.F82I
EPX	58193836	58193836	Splice_Region	G	G	A	rs115633369	S16	
ZNF625	12147388	12147388	Splice_Region	G	G	A		S16	
FCGBP	39899549	39899549	Splice_Region	C	C	T	rs1157993436	S16	
MUC3A	1.01E+08	1.01E+08	Splice_Region	G	G	A	rs75534608	S16	
SLC66A1	19317792	19317792	Missense	G	G	A	rs766989390	S17	p.V39M
PUM1	30953712	30953712	Splice_Site	A	A	G		S17	p.X900_splice

NBPF12	1.47E+08	1.47E+08	Missense	A	A	T	rs1553886396	S17	p.N492I
NBPF11	1.48E+08	1.48E+08	Missense	T	C	C	rs57784339	S17	p.N53S
OR13A1	45304502	45304502	Splice_Site	T	T	G	rs10900195	S17	
OR10AG1	55968031	55968031	Missense	G	G	T		S17	p.P165T
FMNL1	45245100	45245100	Missense	C	C	T		S17	p.A907V
LILRB2	54279040	54279040	Missense	G	G	A	rs1473278082	S17	p.L243F
SCN5A	38581265	38581265	Missense	C	C	T	rs199473181	S17	p.R965H
SRA1	1.41E+08	1.41E+08	Splice_Region	GGT	GGT	A	rs1554096269	S17	
NDST4	1.15E+08	1.15E+08	Missense	C	C	T	rs764667030	S17	p.R708Q
SPEF2	35700537	35700537	Missense	C	C	T	rs938738108	S17	p.P728L
SRA1	1.41E+08	1.41E+08	In_Frame_Ins	C	C	GTCG	rs368142622	S17	p.V110delinsRL
HLA-DRB5	32530124	32530124	Splice_Site	C	C	G	rs79192142	S17	p.X34_splice
BRAF	1.41E+08	1.41E+08	Missense	A	A	T	rs113488022	S17	p.V640E
UNC13B	35295830	35295830	Nonsense	C	C	T	rs146675814	S17	p.R221*
AJM1	1.37E+08	1.37E+08	Missense	C	C	T		S17	p.L814F
NBPF11	1.48E+08	1.48E+08	Missense	T	T	C	rs57784339	S19	p.N53S
OR13A1	45304502	45304502	Splice_Site	T	G	G	rs10900195	S19	
APPL2	1.05E+08	1.05E+08	Missense	G	G	A	rs757933124	S19	p.R537C
VWA8	41575814	41575814	Missense	C	C	T		S19	p.D1766N
ANKS3	4727086	4727086	Missense	G	G	C		S19	p.L88V
UTP6	31889326	31889326	Missense	C	C	A	rs199527189	S19	p.A168S
LILRB2	54279040	54279040	Missense	G	G	A	rs1473278082	S19	p.L243F
SPHKAP	2.28E+08	2.28E+08	Missense	G	G	T		S19	p.S1273R
CTNNB1	41224606	41224606	Missense	G	G	T	rs28931588	S19	p.D32Y
TRIM42	1.41E+08	1.41E+08	Missense	C	C	T		S19	p.R228C
CARD6	40843710	40843710	Splice_Site	G	G	A	rs770198619	S19	p.X281_splice
SRA1	1.41E+08	1.41E+08	Splice_Region	GGT	GGT	A	rs1554096269	S19	
HLA-DRB5	32522178	32522178	Splice_Region	T	T	G	rs36153736	S19	
SRA1	1.41E+08	1.41E+08	In_Frame_Ins	C	C	GTCG	rs368142622	S19	p.V110delinsRL
DOCK2	1.7E+08	1.7E+08	Missense	G	G	A	rs780312697	S19	p.R1370Q

BACH2	89950463	89950463	Missense	G	G	A	rs756865203	S19	p.S548L
DDC	50463334	50463334	Missense	C	C	A		S19	p.R447L
BRAF	1.41E+08	1.41E+08	Missense	A	A	T	rs113488022	S19	p.V640E
TAF9B	78138864	78138864	Missense	G	C	C		S19	p.Q38E
DENND2C	1.15E+08	1.15E+08	Missense	C	C	G		S26	p.D651H
OR13A1	45304502	45304502	Splice_Site	T	G	G	rs10900195	S26	
OR9I1	58119080	58119080	Missense	C	C	T	rs769620522	S26	p.R122H
ZNF705E	71819721	71819721	Nonsense	C	C	T	rs11235129	S26	p.W21*
NCOR2	1.24E+08	1.24E+08	Missense	G	G	A	rs1310731588	S26	p.R1537W
FCGBP	39899549	39899549	Splice_Region	C	C	T	rs1157993436	S26	
PDIA2	285548	285548	Missense	G	G	A	rs199881504	S26	p.V322M
LILRB2	54279040	54279040	Missense	G	G	A	rs1473278082	S26	p.L243F
PAK2	1.97E+08	1.97E+08	Missense	C	C	G		S26	p.I111M
CEP72	653055	653055	Missense	G	G	A	rs777894377	S26	p.E616K
TINAG	54308696	54308696	Missense	G	G	C	rs995476692	S26	p.R49T
DNAJC30	73683218	73683218	Missense	T	T	G		S26	p.Y69S
SMO	1.29E+08	1.29E+08	Missense	C	C	T	rs879255280	S26	p.L412F
SYK	90862228	90862228	Missense	G	G	A	rs769228620	S26	p.G201S
NBPF11	1.48E+08	1.48E+08	Missense	T	T	C	rs57784339	S29	p.N53S
OR13A1	45304502	45304502	Splice_Site	T	T	G	rs10900195	S29	
OR5BS1P	48560442	48560442	Missense	G	G	C	rs7312017	S29	p.L187F
TBXA2R	3600436	3600436	Missense	G	G	C		S29	p.L67V
LILRB2	54279040	54279040	Missense	G	G	A	rs1473278082	S29	p.L243F
VWA3B	98192975	98192975	Missense	C	C	T	rs770917627	S29	p.T515M
ABCF3	1.84E+08	1.84E+08	Missense	C	C	T	rs748060492	S29	p.R204C
AK9	1.1E+08	1.1E+08	Missense	C	C	T	rs963089296	S29	p.G1617R
RPS6KA2	1.66E+08	1.66E+08	Missense	G	G	A	rs779109340	S29	p.R515C
BRAF	1.41E+08	1.41E+08	Missense	A	A	T	rs113488022	S29	p.V640E
TEK	27206741	27206741	Missense	C	C	T	rs147231791	S29	p.R842C
TGFBR1	99137927	99137927	Nonsense	C	C	T		S29	p.R219*

FCGBP	39899549	39899549	Splice_Region	C	C	T	rs1157993436	S29	
NBPF12	1.47E+08	1.47E+08	Missense	A	A	T	rs1553886396	S30	p.N492I
OR13A1	45304502	45304502	Splice_Site	T	T	G	rs10900195	S30	
ZNF705E	71819721	71819721	Nonsense	C	C	T	rs11235129	S30	p.W21*
RESF1	31981485	31981485	Missense	C	C	T	rs1428915741	S30	p.P177L
KRT18	52949447	52949447	Missense	G	G	C	rs1434610693	S30	p.A92P
JMJD7-PLA2G4B	41846783	41846783	Missense	G	G	T		S30	p.R863L
LILRB2	54279040	54279040	Missense	G	G	A	rs1473278082	S30	p.L243F
KIR2DL1	54775384	54775384	Missense	G	G	C	rs371438548	S30	p.R197T
SEC24D	1.19E+08	1.19E+08	Missense	C	C	T	rs1235485163	S30	p.E357K
HLA-DRB5	32530124	32530124	Splice_Site	C	C	G	rs79192142	S30	p.X34_splice
ANKRD30A	37145060	37145060	Splice_Region	T	T	C	rs200031600	S30	
SFXN2	1.03E+08	1.03E+08	Splice_Region	C	C	T		S30	
FCGBP	39899549	39899549	Splice_Region	C	C	T	rs1157993436	S30	
MUC3A	1.01E+08	1.01E+08	Splice_Region	G	G	A	rs75534608	S30	
BRAF	1.41E+08	1.41E+08	Missense	A	A	T	rs113488022	S30	p.V640E
DLC1	13100251	13100251	Missense	C	C	T	rs746121142	S30	p.G696R
CYP4X1	47033264	47033264	Missense	G	G	A	rs751911913	S31	p.G130R
IFITM5	299306	299306	Missense	T	T	G		S31	p.K62T
SIRT4	1.2E+08	1.2E+08	Missense	G	G	A	rs916643694	S31	p.G162R
CRYGC	2.08E+08	2.08E+08	Splice_Region	C	C	T	rs144850837	S31	
HMGN3	79208547	79208547	Splice_Region	C	C	T	rs765210736	S31	p.A32=
MUC3A	1.01E+08	1.01E+08	Splice_Region	G	G	A	rs75534608	S31	
GAN	81356956	81356956	Missense	C	C	T	rs776397915	S31	p.R269W
LILRB2	54279040	54279040	Missense	G	G	A	rs1473278082	S31	p.L243F
PRR5-ARHGAP8	44802122	44802122	Missense	G	G	A	rs181719747	S31	p.R296Q

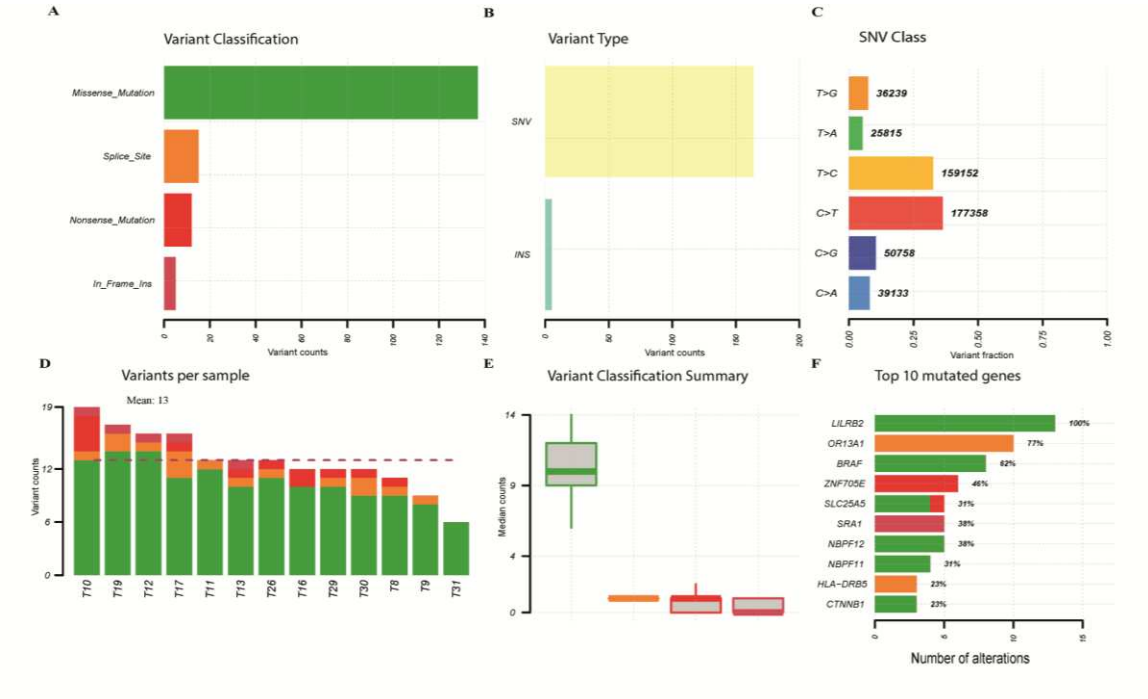

Supplementary Figure S2: Summary of the somatic mutational landscape of ameloblastoma

In A, missense mutations represented the most common type, with almost ~140 variants across the cohort, followed by splice site, nonsense mutations and in-frame insertions with less than ~10 variants. B and C shows that single nucleotide variants (SNV) were the most common variant type, and the C > T transition was the most common class among the six types of base conversions. D shows the mutational load per sample, and the line displays the mean number of variants across the cohort, with a median of 13 variants per sample. In E, the box plots represent the variant classification summary across the 13 tumor samples. In F, the most frequently mutated genes across the cohort.

Supplementary Table S5: Enriched GO gene sets from the analysis of the 13 whole-exome sequenced tumors and their biological process

Cluster	GO	Biological Process
Regulation of Immune Response	:0002764	immune response-regulating signaling pathway
	:0002768	immune response-regulating cell surface receptor signaling pathway
Regulation of apoptotic process	:0006915	apoptotic process
	:0043069	negative regulation of programmed cell death
	:0043066	negative regulation of apoptotic process
	:0043067	regulation of programmed cell death
	:0010941	regulation of cell death
	:0042981	regulation of apoptotic process

Regulation of nucleobase-containing compound metabolic process	:0010558	negative regulation of macromolecule biosynthetic process
	:0009890	negative regulation of biosynthetic process
	:2000113	negative regulation of cellular macromolecule biosynthetic process
	:0045892	negative regulation of transcription, DNA-templated
	:0031327	negative regulation of cellular biosynthetic process
	:1902679	negative regulation of RNA biosynthetic process
	:0051253	negative regulation of RNA metabolic process
	:1903507	negative regulation of nucleic acid-templated transcription
	:0045934	negative regulation of nucleobase-containing compound metabolic process
Regulation of cell differentiation and developmental processes	:0045596	negative regulation of cell differentiation
	:0045595	regulation of cell differentiation
	:0051093	negative regulation of developmental process
Regulation of cell population proliferation	:0042127	regulation of cell population proliferation
	:0008283	cell population proliferation
	:0008284	positive regulation of cell population proliferation
Regulation of cell adhesion	:0007156	homophilic cell adhesion via plasma membrane adhesion molecules

Supplementary Table S6: KEGG pathways from PPIs between somatic variants in ameloblastoma

KEGG Pathway	size	pValue	FDR	Genes
ErbB signaling pathway	85	8.77896E-05	0.028619	BRAF;ERBB3;PIK3R1;AKT1;HBEGF;PAK2
Osteoclast differentiation	128	0.000813592	0.076952	CSF1R;PIK3R1;AKT1;LILRB2;SYK;TGFBR1
Colorectal cancer	86	0.000864409	0.076952	BRAF;CTNNB1;PIK3R1;AKT1;TGFBR1
MAPK signaling pathway	295	0.000944197	0.076952	BRAF;CSF1R;ERBB3;AKT1;PAK2;RPS6KA2;TEK;TGFBR1;JMJD7-PLA2G4B
Endometrial cancer	58	0.001558323	0.091131	BRAF;CTNNB1;PIK3R1;AKT1
Proteoglycans in cancer	201	0.001708948	0.091131	BRAF;CTNNB1;ERBB3;PIK3R1;SMO;AKT1;HBEGF
Acute myeloid leukemia	66	0.002513207	0.091131	BRAF;CSF1R;PIK3R1;AKT1

Non-small cell lung cancer	66	0.002513207	0.091131	BRAF;PIK3R1;ALK;AKT1
Fc epsilon RI signaling pathway	68	0.00280323	0.091131	PIK3R1;AKT1;SYK;JMJD7-PLA2G4B
Renal cell carcinoma	69	0.002956507	0.091131	BRAF;PIK3R1;AKT1;PAK2

Supplementary Table S7: Cancer driver list genes according to Cancer Genome Interpreter

Symbol	Alt	Ref	Sample	Type	Protein change	Oncogenic classification	Consequence
NCOR2	A	G	S26	SNV	R1537W	predicted	missense_variant
KMT2D	A	G	S16	SNV	Q3293*	predicted	stop_gained
KMT2D	G	-	S30	INS	P647PX	predicted	frameshift_variant
KMT2D	T	G	S9	SNV	Y389*	predicted	stop_gained
ERBB3	A	G	S13	SNV	R106Q	predicted	missense_variant
WNK1	G	C	S29	SNV	L1583V	predicted	missense_variant
PABPC3	ACT	GCC	S10	MNV	RL206-207HF	predicted	missense_variant
PABPC3	ACT	GCC	S11	MNV	RL206-207HF	predicted	missense_variant
PABPC3	ACT	GCC	S13	MNV	RL206-207HF	predicted	missense_variant
PABPC3	ACT	GCC	S16	MNV	RL206-207HF	predicted	missense_variant
PABPC3	ACT	GCC	S17	MNV	RL206-207HF	predicted	missense_variant
PABPC3	ACT	GCC	S30	MNV	RL206-207HF	predicted	missense_variant
PABPC3	ACT	GCC	S31	MNV	RL206-207HF	predicted	missense_variant
PABPC3	-	A	S31	DEL	K333X	predicted	frameshift_variant
AKT1	T	C	S10	SNV	E17K	known driver	missense_variant
CHD8	T	C	S16	SNV	R1828H	predicted	missense_variant
OCA2	G	A	S12	SNV	I477T	predicted	missense_variant
SIN3A	C	T	S29	SNV	N735S	predicted	missense_variant
ERCC4	A	G	S26	SNV	R692Q	predicted	missense_variant
WRAP53	A	G	S10	SNV	R398Q	predicted	missense_variant
SERPINB3	CCACC	-	S16	INS	G351GWX	predicted	frameshift_variant
SERPINB3	CCACC	-	S26	INS	G351GWX	predicted	frameshift_variant
SERPINB3	CCACC	-	S29	INS	G351GWX	predicted	frameshift_variant

SERPINB3	CCACC	-	S30	INS	G351GWX	predicted	frameshift_variant
SERPINB3	CCACC	-	S31	INS	G351GWX	predicted	frameshift_variant
SERPINB3	CCACC	-	S8	INS	G351GWX	predicted	frameshift_variant
MUC16	TG	CA	S11	MNV	C12718H	predicted	missense_variant
MUC16	TG	CA	S12	MNV	C12718H	predicted	missense_variant
MUC16	TG	CA	S8	MNV	C12718H	predicted	missense_variant
MUC16	TG	CA	S9	MNV	C12718H	predicted	missense_variant
ASPM	CC	TA	S19	MNV	L2522W	predicted	missense_variant
ARID1A	G	C	S16	SNV	Y212*	predicted	stop_gained
CLSPN	-	TCC	S31	DEL	EE996-997E	predicted	inframe_deletion
GFI1	A	G	S12	SNV	R415W	predicted	missense_variant
SIRPA	ATCA	GTTG	S12	MNV	VL43-44VS	predicted	missense_variant
SIRPA	ATCA	GTTG	S13	MNV	VL43-44VS	predicted	missense_variant
SIRPA	ATCA	GTTG	S19	MNV	VL43-44VS	predicted	missense_variant
SIRPA	ATCA	GTTG	S26	MNV	VL43-44VS	predicted	missense_variant
SIRPA	ATCA	GTTG	S29	MNV	VL43-44VS	predicted	missense_variant
SIRPA	ATCA	GTTG	S30	MNV	VL43-44VS	predicted	missense_variant
SIRPA	ATCA	GTTG	S31	MNV	VL43-44VS	predicted	missense_variant
PLXNB2	T	C	S9	SNV	V151M	predicted	missense_variant
ALK	T	C	S10	SNV	V349I	predicted	missense_variant
LRPPRC	C	T	S9	SNV	Y714C	predicted	missense_variant
CAPN7	A	G	S13	SNV	R343K	predicted	missense_variant
CTNNB1	T	G	S19	SNV	D32Y	known driver	missense_variant
CTNNB1	A	C	S12	SNV	S33Y	known driver	missense_variant
CTNNB1	G	C	S13	SNV	S33C	known driver	missense_variant
CSF1R	T	C	S11	SNV	A770T	predicted	missense_variant
FAT2	A	G	S19	SNV	T3200M	predicted	missense_variant
PIK3R1	-	TAA	S29	DEL	LI404-405L	predicted	inframe_deletion
LNPEP	A	G	S8	SNV	R89Q	predicted	missense_variant
MCM3	A	T	S29	SNV	D325V	predicted	missense_variant
BRAF	T	A	S10	SNV	V600E	known driver	missense_variant
BRAF	T	A	S11	SNV	V600E	known driver	missense_variant
BRAF	T	A	S12	SNV	V600E	known driver	missense_variant
BRAF	T	A	S17	SNV	V600E	known driver	missense_variant

BRAF	T	A	S19	SNV	V600E	known driver	missense_variant
BRAF	T	A	S29	SNV	V600E	known driver	missense_variant
BRAF	T	A	S30	SNV	V600E	known driver	missense_variant
BRAF	T	A	S9	SNV	V600E	known driver	missense_variant
SVEP1	CA	TG	S10	MNV	A2753V	predicted	missense_variant
SVEP1	CA	TG	S12	MNV	A2753V	predicted	missense_variant
SVEP1	CA	TG	S13	MNV	A2753V	predicted	missense_variant
SVEP1	CA	TG	S16	MNV	A2753V	predicted	missense_variant
SVEP1	CA	TG	S17	MNV	A2753V	predicted	missense_variant
SVEP1	CA	TG	S19	MNV	A2753V	predicted	missense_variant
SVEP1	CA	TG	S26	MNV	A2753V	predicted	missense_variant
SVEP1	CA	TG	S29	MNV	A2753V	predicted	missense_variant
SVEP1	CA	TG	S30	MNV	A2753V	predicted	missense_variant
SVEP1	CA	TG	S31	MNV	A2753V	predicted	missense_variant
SVEP1	CA	TG	S8	MNV	A2753V	predicted	missense_variant
SVEP1	CA	TG	S9	MNV	A2753V	predicted	missense_variant
SVEP1	A	G	S16	SNV	P1036S	predicted	missense_variant
BCOR	A	G	S16	SNV	Q1441*	predicted	stop_gained
ATP6AP2	T	A	S9	SNV	N308Y	predicted	missense_variant

Alt: alternative allele; Ref: reference allele; SNV: single nucleotide variation; INS: insertion; MNV: multi-nucleotide variant ; DEL: deletion

Supplementary Table S8: Signalling and related pathways affecting Cancer Driver Genes in ameloblastoma

Gene	Signaling or related pathway/GO annotations
BRAF	MAPK/ERK
KMT2D	RNA Polymerase I Promoter Opening and Gene Expression (Transcription)
CTNNB1	Wnt/β-catenin
ARID1A	Gene expression and Chromatin organization/ binding and nuclear receptor binding
ATP6AP2	Innate Immune System/ enzyme binding as aspartic-type endopeptidase activity
BCOR	Ectoderm differentiation/ *transcription factor binding* and *transcription cis-regulatory region binding*
CSF1R	GPCR Pathway and ERK Signalling/ protein homodimerization and protein kinase activity
ERBB3	GPCR Pathway and Prolactin Signalling/ protein homodimerization and transferase activity
ERCC4	DNA repair pathways/ nucleic acid binding
GFI1	RNA polymerase I promotor opening/ DNA-binding transcription repressor
LNPEP	Class I MHC mediated antigen processing/ metallopeptidase activity and aminopeptidase activity
PIK3R1	IL9 Signalling Pathways/ GTP binding and transcription factor binding
SIN3A	RNA Polymerase I Promoter Opening/ DNA-binding transcription factor activity

WRAP53	Chromosome Maintenance/ RNA binding
ALK	GPCR Pathway/ Protein kinase activity
CAPN7	Extracellular matrix organization/ endopeptidase activity
CHD8	ncRNAs involved in Wnt signaling in hepatocellular carcinoma and Signalling by WNT7 nucleic acid binding
FAT2	No information
LRPPRC	TP53 Regulates Metabolic Genes and Gene Expression (Transcription).
MCM3	Mitotic G1 phase and G1/S transition and Activation of the pre-replicative complex
NCOR	Transcriptional activation of mitochondrial biogenesis
OCA2	Regulation of expression of SLITs and ROBOs
PLXNB2	No information
WNK1	PI3K / Akt Signalling
SMO	Hedgehog Signalling
AKT1	PI3K / Akt Signalling

GPCR: G-protein-coupled receptors. Information about signaling/related pathways was taken out from GeneCards (https://www.genecards.org/).

Supplementary Table S9: Coverage tracks information on the candidate variants

Sample	Gene symbol	AA Change	Ref: Alt	Total count (DP)	Ref count: Alt count	Ref %: Alt %	Genotype
T12	*CTNNB1*	S33Y	C: A	380	299: 81	78: 22	het
T13	*CTNNB1*	S33C	C: G	324	216: 107	67: 33	het
T19	*CTNNB1*	D32Y	G: T	297	164: 133	55: 45	het
T10	*BRAF*	V600E	A: T	137	80: 57	58: 42	het
T11	*BRAF*	V600E	A: T	101	57: 44	56: 44	het
T12	*BRAF*	V600E	A: T	119	90: 29	75: 24	het
T17	*BRAF*	V600E	A: T	123	78: 45	63: 37	het
T19	*BRAF*	V600E	A: T	83	57: 26	69: 31	het
T29	*BRAF*	V600E	A: T	148	75: 73	51: 49	het
T30	*BRAF*	V600E	A: T	130	78: 52	60: 40	het
T9	*BRAF*	V600E	A: T	122	75: 47	61: 39	het
T16	*KMT2D*	Q3293X	G: A	78	42: 36	54: 46	het
T30	*KMT2D*	P648Tfs*1	-: G	36	18: 18	50:50	het
T9	*KMT2D*	Y389X	G: T	116	78: 38	67: 33	het

Ref: Alt: reference and alternative alleles; DP: read depth; het: heterozygous.

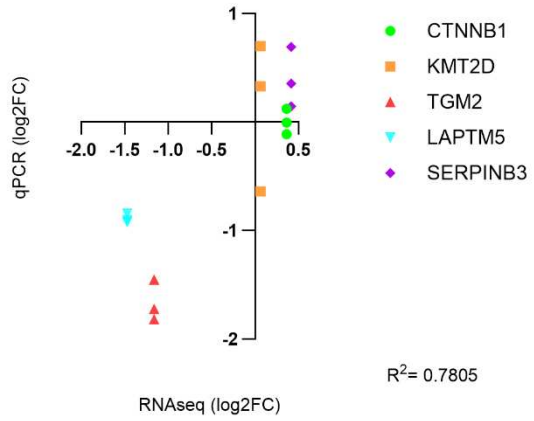

Supplementary Figure S3: qPCR vs RNA-sequencing agreement

RNA-sequencing (log2FC, X axis) of the candidate genes plotted against the results of the qPCR assays (log2FC, Y axis). There was a high correlation in the measurement of both gene expression quantification platforms for the tumors, as shown in the scatterplot.

Supplementary Table S10: List of genes from the hallmark epithelial-mesenchymal transition enriched in cluster 1

SYMBOL	RANK IN GENE LIST	RANK METRIC SCORE	RUNNING ES
SNTB1	209	0.913005531	0.003275356
SLIT3	222	0.90327996	0.014268934
SGCD	312	0.832966864	0.021304525
PMEPA1	365	0.799075067	0.02938252
COL7A1	399	0.77725935	0.037939772
MSX1	520	0.721949518	0.042331517
MMP3	555	0.707076013	0.049957667
IGFBP3	619	0.689990044	0.056212466
WIPF1	620	0.689832449	0.06497303
ELN	646	0.682065547	0.07263981
COL5A3	713	0.665070891	0.07845873
CALU	796	0.646261096	0.08340188
P3H1	923	0.616696477	0.08621812
MYLK	934	0.614918709	0.093629256
IGFBP4	963	0.610043705	0.10026197
DPYSL3	1010	0.601445138	0.10606899
CDH11	1022	0.599106073	0.113239504
GPC1	1053	0.590260565	0.11954137
DAB2	1121	0.577331364	0.12420624
THY1	1194	0.565090656	0.12851661
FSTL1	1198	0.564472079	0.13556574
COL5A2	1205	0.563429058	0.1424822
EMP3	1273	0.551567018	0.14681987
PDGFRB	1340	0.5390324	0.15103815

COL6A3	1415	0.527513385	0.15479171
LRP1	1465	0.52065295	0.15945329
VCAN	1517	0.512725115	0.16393457
POSTN	1532	0.510902166	0.16986552
OXTR	1551	0.507991791	0.17560028
THBS1	1588	0.503279746	0.1805587
FN1	1618	0.499195546	0.1857439
PRRX1	1623	0.498637766	0.19191714
IL6	1656	0.495060205	0.1969304
TGFBI	1722	0.485212088	0.200505
LOXL2	1831	0.471442401	0.20219308
LAMC1	1877	0.46690616	0.20633133
CALD1	1891	0.463899463	0.21170516
EDIL3	1894	0.463677019	0.21751404
NNMT	2003	0.451274574	0.218946
COL8A2	2033	0.448322654	0.22348513
INHBA	2350	0.436108798	0.2164449
SLIT2	2394	0.433176398	0.2202344
MXRA5	2515	0.426660478	0.2208761
LUM	2550	0.424873203	0.22491841
SPARC	2689	0.415747315	0.22470501
ENO2	2699	0.414479464	0.22961046
PLOD2	2741	0.41184479	0.23320867
FOXC2	2779	0.409525901	0.23693666
COL12A1	2820	0.406412303	0.24050568
COL3A1	2824	0.406197488	0.24554478
NOTCH2	2879	0.40352878	0.24851991
FBLN5	2981	0.397245556	0.24954437
TNC	2996	0.396156907	0.2540181
THBS2	3117	0.386392504	0.25414842
LRRC15	3134	0.385299325	0.25840464
VCAM1	3154	0.384171963	0.26252717
WNT5A	3160	0.383868754	0.2672031
CD44	3201	0.38114956	0.27045128
TIMP3	3242	0.378356516	0.273664
ABI3BP	3256	0.37772274	0.27794343
SERPINE2	3342	0.371986538	0.279284
TPM1	3378	0.370145977	0.2825915
TGFBR3	3574	0.356511652	0.27935693
ADAM12	3585	0.356111407	0.2834813
LOX	3622	0.35346821	0.2865372
ANPEP	3626	0.353334069	0.29090497
PLOD1	3722	0.34654218	0.29152435
FBLN1	3724	0.346457809	0.2958844
PMP22	3804	0.343075007	0.29709664
COL1A2	3829	0.340820938	0.30046958

GPX7	3834	0.340384245	0.30463308
NID2	3853	0.339507282	0.30822816
DCN	3911	0.335903734	0.31022507
CCN2	4026	0.327746212	0.30984944
COL11A1	4088	0.324023366	0.31153622
VIM	4097	0.32332924	0.31532392
COL5A1	4261	0.310560375	0.31277955
ID2	4287	0.308931082	0.3157077
FBN1	4290	0.308774471	0.31954938
LOXL1	4438	0.297874749	0.3174808
ITGB3	4450	0.297004521	0.3208148

Supplementary Table S11: Enriched sets in BRAF WT using the MSigDB Hallmark gene sets collection

Name	Size	p-val	FDR	Process Category
HALLMARK_ALLOGRAFT_REJECTION	200	0	0	immune
HALLMARK_TNFA_SIGNALING_VIA_NFKB	200	0	0	signaling
HALLMARK_INFLAMMATORY_RESPONSE	200	0	0	immune
HALLMARK_IL6_JAK_STAT3_SIGNALING	87	0	4.03E-04	immune
HALLMARK_INTERFERON_GAMMA_RESPONSE	200	0	3.22E-04	immune
HALLMARK_KRAS_SIGNALING_UP	200	0	0.003587	signaling
HALLMARK_UV_RESPONSE_DN	144	0.002551	0.024805	DNA damage
HALLMARK_EPITHELIAL_MESENCHYMAL_TRANSITION	200	0.002427	0.027266	development
HALLMARK_COMPLEMENT	200	0.003606	0.043232	immune
HALLMARK_INTERFERON_ALPHA_RESPONSE	97	0.034916	0.080287	immune
HALLMARK_IL2_STAT5_SIGNALING	199	0.019827	0.103114	signaling
HALLMARK_MYOGENESIS	200	0.041147	0.166989	development

The size column indicates the number of genes represented in each gene set.

Supplementary Table S12: Analysis of gene fusions in ameloblastoma

Sample	Fusion Name (5´- 3´)	5´Breakpoint Position (chr:nt)	3´Breakpoint Position (chr:nt)
T10	RACK1--RPL27	chr5:181239510:-	chr17:43002872:+
T16	PANCR--AC098798.1	chr4:110615307:-	11092
T16	RPL17--PSMG2	chr18:49489359:-	16863
T16	AC121154.1--AC108075.1	chr4:124251992:-	9718
T17	PANCR--AC098798.1	chr4:110615307:-	11092
T17	COPA--SPCS1	chr1:160289579:-	34488
T17	SUZ12P1--CRLF3	chr17:30769965:+	35955
T17	GMIP--WAS	chr19:19641810:-	23337
T19	PANCR--AC098798.1	chr4:110615307:-	chr4:110513539:-
T19	SAA4--SAA1	chr11:18232395:-	chr11:18269717:+
T19	RNF152--AC105094.2	chr18:61892795:-	chr18:61592623:-
T26	SAA4--SAA1	chr11:18232395:-	chr11:18269717:+
T26	PCNP--ADK	chr3:101574279:+	chr10:74670183:+
T26	NOP53--DHX34	chr19:47745783:+	chr19:47381980:+
T26	RPL10--IMPDH2	chrX:154400733:+	chr3:49024746:-
T26	IGH-@-ext--RPS9	chr14:105978763:+	chr19:54207401:+
T30	PANCR--AC098798.1	chr4:110615307:-	chr4:110513539:-
T30	AC121154.1--AC108075.1	chr4:124188144:-	chr4:124025603:-
T30	RPL13--MFGE8	chr16:89563276:+	chr15:88898801:-
T30	RGS7--MRPS31	chr1:240930717:-	chr13:40729601:-
T30	NR3C1--CBX5	chr5:143281670:-	chr12:54231155:-
T30	H3-3B--IQGAP1	chr17:75777498:-	chr15:90501764:+
T30	AC121154.1--AC108075.1	chr4:124251992:-	chr4:124025603:-
T30	AC092807.3--DDAH1	chr1:85496166:-	chr1:85358847:-

References

1. Raudvere U, Kolberg L, Kuzmin I, Arak T, Adler P, Peterson H, et al. g:Profiler: a web server for functional enrichment analysis and conversions of gene lists (2019 update). Nucleic Acids Res. 2019;47(W1):W191-W8.
2. Shannon P, Markiel A, Ozier O, Baliga NS, Wang JT, Ramage D, et al. Cytoscape: a software environment for integrated models of biomolecular interaction networks. Genome Res. 2003;13(11):2498-504.